

Accurate Modeling of Ionospheric Electromagnetic Fields Generated by a Low-Altitude VLF Transmitter

Steven A. Cummer

**Duke University
130 Hudson Hall
Box 90291
Durham, NC 27708**

Scientific Report No. 2

31 August 2007

APPROVED FOR PUBLIC RELEASE; DISTRIBUTION UNLIMITED.



**AIR FORCE RESEARCH LABORATORY
Space Vehicles Directorate
29 Randolph Road
AIR FORCE MATERIEL COMMAND
Hanscom AFB, MA 01731-3010**

NOTICE AND SIGNATURE PAGE

Using Government drawings, specifications, or other data included in this document for any purpose other than Government procurement does not in any way obligate the U.S. Government. The fact that the Government formulated or supplied the drawings, specifications, or other data does not license the holder or any other person or corporation; or convey any rights or permission to manufacture, use, or sell any patented invention that may relate to them.

This report was cleared for public release and is available to the general public, including foreign nationals. Qualified requestors may obtain additional copies from the Defense Technical Information Center (DTIC) (<http://www.dtic.mil>). All others should apply to the National Technical Information Service.

AFRL-RV-HA-TR-2007-1137 HAS BEEN REVIEWED AND IS APPROVED FOR
PUBLICATION IN ACCORDANCE WITH ASSIGNED DISTRIBUTION STATEMENT.

//Signature//

MICHAEL STARKS
Contract Manager

//Signature//

JOEL MOZER, Chief
Space Weather Center of Excellence

This report is published in the interest of scientific and technical information exchange, and its publication does not constitute the Government's approval or disapproval of its ideas or findings.

REPORT DOCUMENTATION PAGE				Form Approved OMB No. 0704-0188	
Public reporting burden for this collection of information is estimated to average 1 hour per response, including the time for reviewing instructions, searching existing data sources, gathering and maintaining the data needed, and completing and reviewing this collection of information. Send comments regarding this burden estimate or any other aspect of this collection of information, including suggestions for reducing this burden to Department of Defense, Washington Headquarters Services, Directorate for Information Operations and Reports (0704-0188), 1215 Jefferson Davis Highway, Suite 1204, Arlington, VA 22202-4302. Respondents should be aware that notwithstanding any other provision of law, no person shall be subject to any penalty for failing to comply with a collection of information if it does not display a currently valid OMB control number. PLEASE DO NOT RETURN YOUR FORM TO THE ABOVE ADDRESS.					
1. REPORT DATE (DD-MM-YYYY) 31-08-2007		2. REPORT TYPE Scientific Report No. 2		3. DATES COVERED (From - To) 08-02-2006 to 08-31-2007	
4. TITLE AND SUBTITLE Accurate Modeling of Ionospheric Electromagnetic Fields Generated by a Low-Altitude VLF Transmitter				5a. CONTRACT NUMBER FA8718-05-C-0052	
				5b. GRANT NUMBER	
				5c. PROGRAM ELEMENT NUMBER 62601F	
6. AUTHOR(S) S. A. Cummer				5d. PROJECT NUMBER 1010	
				5e. TASK NUMBER RR	
				5f. WORK UNIT NUMBER A1	
7. PERFORMING ORGANIZATION NAME(S) AND ADDRESS(ES) Duke University 130 Hudson Hall Box 90291 Durham, NC 27708				8. PERFORMING ORGANIZATION REPORT NUMBER	
9. SPONSORING / MONITORING AGENCY NAME(S) AND ADDRESS(ES) Air Force Research Laboratory 29 Randolph Road Hanscom AFB, MA 01731-3010				10. SPONSOR/MONITOR'S ACRONYM(S) AFRL/VSBXI	
				11. SPONSOR/MONITOR'S REPORT NUMBER(S) AFRL-RV-HA-TR-2007-1137	
12. DISTRIBUTION / AVAILABILITY STATEMENT Approved for Public Release; Distribution Unlimited.					
13. SUPPLEMENTARY NOTES					
20100412131					
14. ABSTRACT The goal of this project is accurate prediction of high-altitude fields generated by low-altitude VLF sources to understand their influence on radiation belt dynamics. We applied a full-wave finite difference numerical model of the electromagnetic fields to compute the VLF energy injected through an arbitrary and, therefore, realistic ionosphere for a source located anywhere on the globe. A complete end-to-end run of the high-altitude VLF power prediction model has been completed using our modeled 130-km altitude VLF power predictions as the input to the higher altitude ray-tracing code. This resulted in good agreement with high-altitude VLF field measurements from the IMAGE satellite. A series of simulations using parameters corresponding to the NML (high latitude) and NPM (low latitude) transmitters showed that, for a given uniform grid spacing, the low-altitude fields can be computed correctly while the high-altitude fields are incorrect. This shows that a nonuniform grid approach, in which low altitudes are resolved coarsely and only the highest altitudes are resolved finely, is the key to achieving efficient simulations of high-altitude fields. Comparisons with results from the time domain code show that our preliminary frequency domain code gives answers in quantitative agreement with the time domain code but is about 90 times faster for single-frequency computations.					
15. SUBJECT TERMS Radiation belt dynamics, Finite-difference-time-domain method, Wave energy injection					
16. SECURITY CLASSIFICATION OF:			17. LIMITATION OF ABSTRACT	18. NUMBER OF PAGES	19a. NAME OF RESPONSIBLE PERSON
a. REPORT	b. ABSTRACT	c. THIS PAGE			Dr. Michael Starks
U	U	U	UU	26	19b. TELEPHONE NUMBER (include area code) 781-377-1486

CONTENTS

1. Summary	1
2. Background and Accomplishments	2
3. Technical Approach	4
3.1. 2D Cylindrical Symmetric FDTD Model	4
3.2. Time Harmonic Modeling	5
4. Primary Results	5
4.1. End-to-End Model Validation	5
4.2. High vs. Low Latitude Model Convergence—Initial Results	7
4.3. High vs. Low Latitude Model Convergence—Complete Analysis	10
4.4. Time Harmonic Code and Initial Results	15
5. Conclusions	19
References	21
List of Symbols, Abbreviations, and Acronyms	22

FIGURES

1. Plot showing the measured NML transmitter VLF electric field measured by IMAGE (red) and the end-to-end model predicted fields (black). The quantitative agreement is excellent and, with our simulations of ionospheric penetration, no ~20-dB empirical correction is required. 6
2. Test of FDTD model convergence from high-latitude NML transmitter. The panels show the spectrum of low-altitude (top) and high-altitude (bottom) electric fields as the grid spacing in the simulation is reduced by 25%. The change in the low-altitude fields is almost negligible across the entire band, indicating that the results are accurate. The high-altitude fields differ somewhat above 20 kHz, but the change is still small. 8
3. Test of FDTD model convergence from low-latitude NPM transmitter. The panels show the spectrum of low-altitude (top) and high-altitude (bottom) electric fields as the grid spacing in the simulation is reduced by 25%. The change in the low-altitude fields is almost negligible across the entire band, indicating that the results are accurate. However, the high-altitude fields differ somewhat above 5 kHz and differ enormously above 15 kHz. 9
4. The low-altitude (90 km) field spectrum for a magnetic latitude corresponding to the NML transmitter (high latitude) for 3 different grid spacings. 11
5. The high-altitude (130 km) field spectrum for a magnetic latitude corresponding to the NML transmitter (high latitude) for 3 different grid spacings. 12
6. The low-altitude (90 km) field spectrum for a magnetic latitude corresponding to the NPM transmitter (low latitude) for 3 different grid spacings. 13
7. The high-altitude (130 km) field spectrum for a magnetic latitude corresponding to the NPM transmitter (low latitude) for 3 different grid spacings. 14
8. Low-altitude fields produced by a 10-kHz source computed using the FD and TD codes. The agreement is excellent, validating the new FD code. 16
9. High-altitude fields produced by a 10-kHz source computed using the FD and TD codes. The agreement is again excellent. 17

10. Low-altitude fields produced by a 20-kHz source computed using the FD and TD codes.

17

11. High-altitude fields produced by a 20-kHz source computed using the FD and TD codes.

18

1. SUMMARY

The main objective of this project is to apply a full-wave electromagnetic field model to predict the injection of wave energy produced by a low-altitude very low frequency (VLF) transmitter through an arbitrary and, therefore, realistic ionosphere. Our specific task is to deliver an accurate model of high-altitude electromagnetic fields and wave energy injection to be used in analyzing and predicting controlled radiation belt particle loss to reduce potential threats to satellite systems. Accurate prediction of high-altitude wave energy injection by low-altitude VLF wave transmission is a challenging but essential step towards accurate modeling of the impact of man-made VLF transmissions on natural radiation belt dynamics. The technical challenge lies in simulating propagation in a lossy, anisotropic and arbitrarily inhomogeneous ionosphere, for which approximate techniques such as ray tracing do not apply.

Our technical approach is to develop a full-wave numerical model to simulate wave power injected into the ionosphere from a ground-level VLF transmitter. The main advantage of a finite difference-based approach is its ability to compute high altitude fields in arbitrary ionospheres, including the influence of Earth's magnetic field, with no implicit approximations.

Our progress in the second year of this project was significantly hindered by delays in receiving funding to support the work. These funding delays also meant that extra time and effort was expended ramping the effort down and back up again. Nevertheless, substantial progress was made. A complete end-to-end run of the high-altitude VLF power prediction model has been completed using our modeled 130-km altitude VLF power predictions as the input to the higher altitude ray-tracing code. This resulted in good agreement with high-altitude VLF field measurements from the IMAGE satellite. Previous end-to-end runs like this, which used semi-empirical ionospheric penetration, had revealed a ~20-dB discrepancy between the measured and predicted fields. Our model does not require any such correction factor and appears to show that this discrepancy originates in the ionospheric penetration calculation.

We have also made significant progress in understanding the convergence of our simulations and, thus, also quantitatively bounding the absolute errors in the results. We have run a series of simulations using parameters corresponding to the NML (high-latitude) and NPM (low-latitude) transmitters with grid spacings of 1000, 500, and 250 meters. Finite difference simulations are guaranteed to eventually converge to the correct answer as this grid spacing is reduced, but it is not always easy to know what grid spacing is required to maintain errors below a specified level. We have found that, for a given uniform grid spacing, the low-altitude fields can be computed correctly while the high-altitude fields are dramatically incorrect. This shows that a nonuniform grid approach, in which low altitudes are resolved coarsely and only the highest altitudes are resolved finely, is the key to achieving efficient simulations of high-altitude fields. At high latitudes (i.e., NML), 500-m grid spacing results in fairly accurate high-altitude fields in the 20–25 kHz band. But at low latitudes (i.e., NPM), 250 m and smaller grid spacing is required to achieve the same accuracy. The convergence in all cases shows

second-order accuracy, which is expected. This also means that correct answers can be estimated by extrapolating the convergence to its limit.

Lastly, the realization that very fine grid spacings are required to achieve accurate results at low latitudes has led us to develop a more efficient frequency domain (i.e., single frequency) VLF solver. Significant progress has been made in developing a more efficient frequency domain solver and validating its accuracy. We have found, and show below, that our preliminary frequency domain code gives answers in quantitative agreement with the time domain code but is about 90 times faster for single-frequency computations. This major enhancement in computational speed justifies the further development needed for this solver.

The ongoing code development will enable accurate predictions of the ionospheric wave fields and their statistical uncertainty. The model output will be designed for easy integration into ray-tracing codes that complete the overall simulation of wave fields in the radiation belts. The end result will be the capability to predict more accurately the injection of VLF wave energy into the magnetosphere, which is a key component in understanding the influence of VLF on radiation belt dynamics.

2. BACKGROUND AND ACCOMPLISHMENTS

Predicting the wave power injected into the magnetosphere from a ground-level VLF or lower frequency transmitter is an essential component in modeling radiation belt dynamics. But accurately computing VLF power penetration through the ionosphere is not easy. Ray tracing, an effective technique in the magnetosphere, is not a good approximation because the ionosphere changes significantly on the scale of a VLF wavelength. Consequently, wave reflection, mode conversion, and other full-wave effects that ray tracing generally neglects are important. Full-wave mode theory techniques [e.g., *Pappert and Ferguson, 1986*] are effective for reliably computing subionospheric fields produced by VLF transmitters. But mode theory techniques are difficult to apply above approximately 60–70 km for realistic ionospheres in which the parameters are not exponentially varying. This upper altitude is too low to be of direct use to the radiation belt problem. Past numerical calculations have been summarized in forms potentially useful for this application, but these calculations have always made assumptions that limit their applicability.

An effective and efficient approach to computing ionospheric VLF fields under very general conditions is full-wave finite difference simulation. This approach contains essentially no approximations other than approximating derivatives as discrete differences. Finite difference techniques, in general, have found wide application in numerical simulations of scattering, propagation, and other electromagnetic phenomena [*Taflove and Hagness, 2000*]. The finite difference technique is well suited to specific aspects of the VLF problem, namely, the relatively long wavelengths involved and a domain with complex inhomogeneities. In fact, it is really the only technique capable of handling the almost completely arbitrary inhomogeneities that appear in the VLF ionospheric penetration problem.

Its chief disadvantage is computational cost; by explicitly computing the electromagnetic fields everywhere in the domain of interest, it is a brute-force approach.

Modern computer speed, however, is sufficient that speed is no longer a major limitation for this class of problem. And, most importantly, we have already developed and validated a code that can compute VLF fields at ionospheric altitudes from an essentially arbitrary source and in an arbitrary ionosphere [Cummer, 2000; Hu and Cummer, 2006]. We have applied this code to short- and long-distance VLF propagation for a variety of ionospheric and lightning remote sensing applications.

The main objective of this work is to deliver a full-wave electromagnetic field model to predict the injection of wave energy produced by a low-altitude VLF transmitter through the ionosphere. Our goal is to accurately model high-altitude fields to better understand radiation belt loss mechanisms and to determine whether they can be modified by VLF wave energy injection at key locations. The work completed during the second year is described below in Section 4.

3. TECHNICAL APPROACH

Terrestrial VLF transmitters play a significant role in the depopulation of energetic particles from the radiation belts. Computing VLF fields in and above the ionosphere from ground transmitters is difficult because wave propagations in a lossy, anisotropic and arbitrarily inhomogeneous ionosphere imply that any approximate techniques such as ray tracing and mode theory for wave simulation are not accurate. Our technique approach is to modify and apply an existing finite difference code to this problem. This code, by approximating derivatives as discrete differences, solves everywhere in the computational domain the Maxwell equations coupled to the equation for vector electric current in a magnetized cold plasma

$$\frac{\partial \mathbf{J}}{\partial t} + \nu \mathbf{J} = \frac{q}{|q|} \omega_b (\mathbf{J} \times \mathbf{b}_E) + \varepsilon_0 \omega_p^2 \mathbf{E},$$

where ω_p is the local plasma frequency, ω_b is the local gyrofrequency, ν is the local collision frequency, and \mathbf{b}_E is the unit vector pointing in the direction of Earth's magnetic field [Budden, 1985]. All of cold plasma magnetoionic theory is contained in these equations and, thus, all relevant physics of linear electromagnetic waves are automatically included in this simulation. For example, the complicated Appleton-Hartree refractive index formula is derived directly from the time harmonic equivalent of the above equation. Both electron and ion effects are included in our model by separately computing the current from each particle species through equations of the same form.

3.1. 2D Cylindrical Symmetric FDTD Modeling

Our primary computational code remains a 2D azimuthally symmetric cylindrical coordinates code. This FDTD code has been developed and carefully validated for years through comparisons with ground measurements and mode theory based LWPC simulations [Hu and Cummer, 2006]. There are several challenges in developing a functional code. The strong anisotropic nature of the medium made simply developing a stable finite difference scheme difficult. Also, the wavelength scales are strongly variable

across the computational domain because the refractive index of the escaping whistler-mode wave energy is very high, leading to very short wavelengths at altitude above 100 km.

3.2. Time Harmonic Modeling

For many of the computations needed for this project, only a single frequency of a small set of frequencies needs to be simulated. A full time domain simulation, which essentially computes all frequencies simultaneously, may be less efficient. Because of the multiscale nature of the problem, in which wavelengths are much shorter in the ionosphere than in the lower altitude free space region, we would like to have variable grid spacing throughout the computational domain. This is difficult to implement in a time domain code, but it is straightforward to implement in a frequency domain or time-harmonic code.

A time-harmonic code is based on a frequency domain representation of the Maxwell equations and governing equations for a cold plasma, in which the time derivatives are converted to complex multiplications by $j\omega$. The equations are approximated by spatial finite differences, and the result is a time-static, matrix equation for all field components at all grid points in the simulation. Although the number of unknowns will be too large for a direct matrix solution, the resulting sparse matrix equation can be solved using any one of a number of classes of iterative sparse matrix solvers.

4. PRIMARY RESULTS

Our technical accomplishments from the second year of our research effort are summarized below.

4.1. End-to-End Model Validation

We ran a careful simulation of the high-altitude (130 km) fields in a 2000-km radius circle around the 25.2-kHz NML transmitter. Our AFRL colleagues used these high-altitude fields as input to a ray-tracing code that computes the VLF power levels at higher altitudes in the magnetosphere. The computed magnetospheric electric field levels were compared to fields measured by the RPI instrument on the IMAGE satellite. Figure 1 shows an example of this comparison. The predicted and measured field levels are in good quantitative agreement with no significant bias towards higher or lower fields. Similarly good agreement was achieved with data from several other IMAGE passes.

These results appear to confirm that the ~20-dB correction factor needed when approximate ionospheric penetration calculations are used originates in the ionospheric penetration calculation itself. Effort is ongoing to confirm this with measurements from other satellites, which would eliminate uncertainty in the measurement calibration as a possible source of the discrepancy. If it holds up, this result means that prior radiation belt loss calculations may need to be revisited in light of weaker ionospheric penetration than that predicted by simplified models.

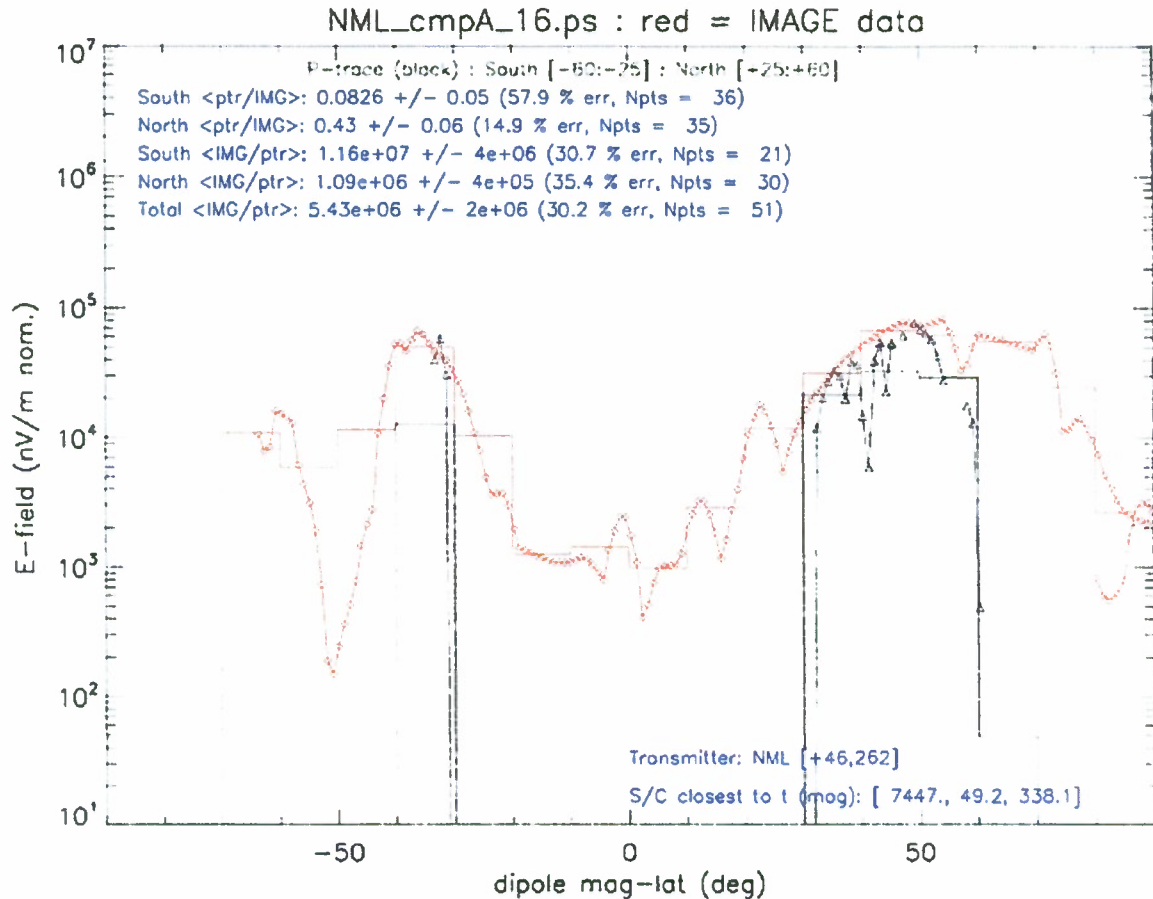


Figure 1. Plot showing the measured NML transmitter VLF electric field measured by IMAGE (red) and the end-to-end model predicted fields (black). The quantitative agreement is excellent and, with our simulations of ionospheric penetration, no ~20-dB empirical correction is required.

4.2. High-Latitude vs. Low-Latitude Model Convergence—Initial Results

As noted in previous reports, simulations are indicating that there is a significant latitude dependence on the numerical parameters needed for accurate simulations. This is demonstrated in Figures 2 and 3, which show initial results in this effort for field computations at the NML and NPM transmitter latitudes, respectively. For both latitudes, we see only minor differences in the low-altitude fields vs. frequency as the grid size is reduced. This confirms that the low-altitude fields are accurate across the entire VLF band for 1-km grid spacing.

However, the high-altitude fields are different. The high-latitude (NML) fields have come close to converging for 0.75-km grid spacing, although a finer grid may be needed for accurate fields above 20 kHz. The low-latitude (NPM) fields, however, are not even close to converged. A modest change in the grid spacing (1 to 0.75 km) increases the fields by more than a factor of 10 above 20 kHz. Clearly, a finer grid spacing is needed for accurate simulations at NPM latitudes.

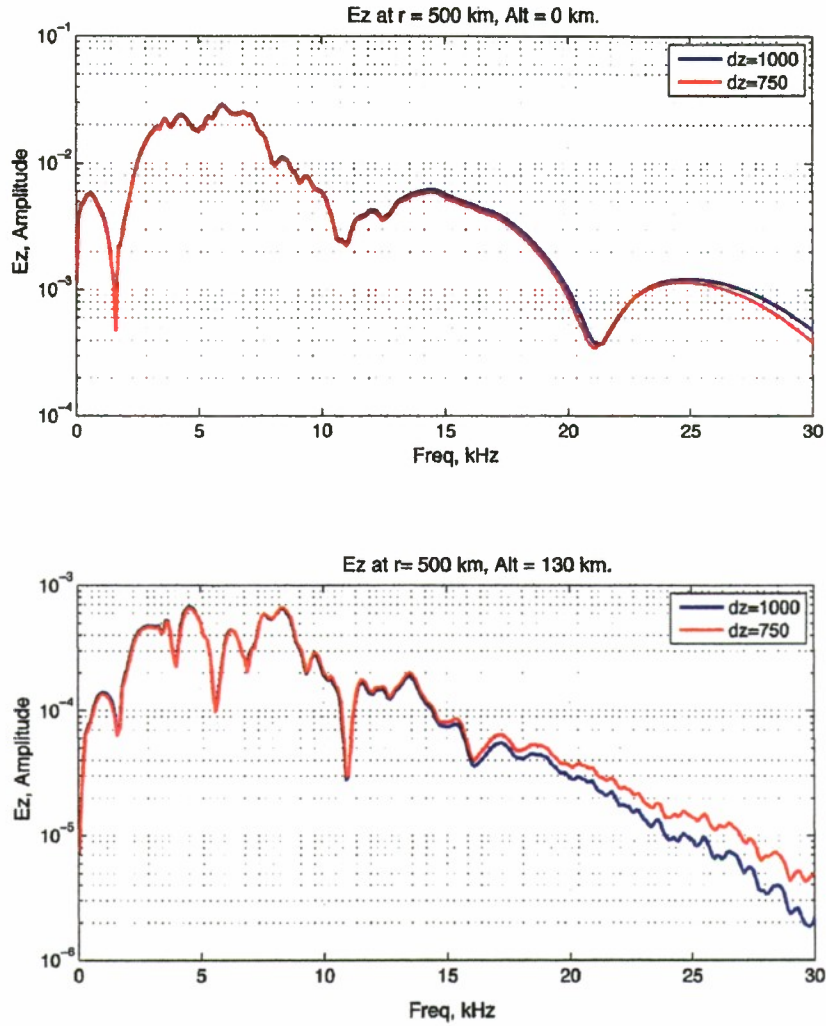


Figure 2. Test of FDTD model convergence from high-latitude NML transmitter. The panels show the spectrum of low-altitude (top) and high-altitude (bottom) electric fields as the grid spacing in the simulation is reduced by 25%. The change in the low-altitude fields is almost negligible across the entire band, indicating that the results are accurate. The high-altitude fields differ somewhat above 20 kHz, but the change is still small. These results indicate that high-latitude fields are correctly computed with 1-km grid spacing.

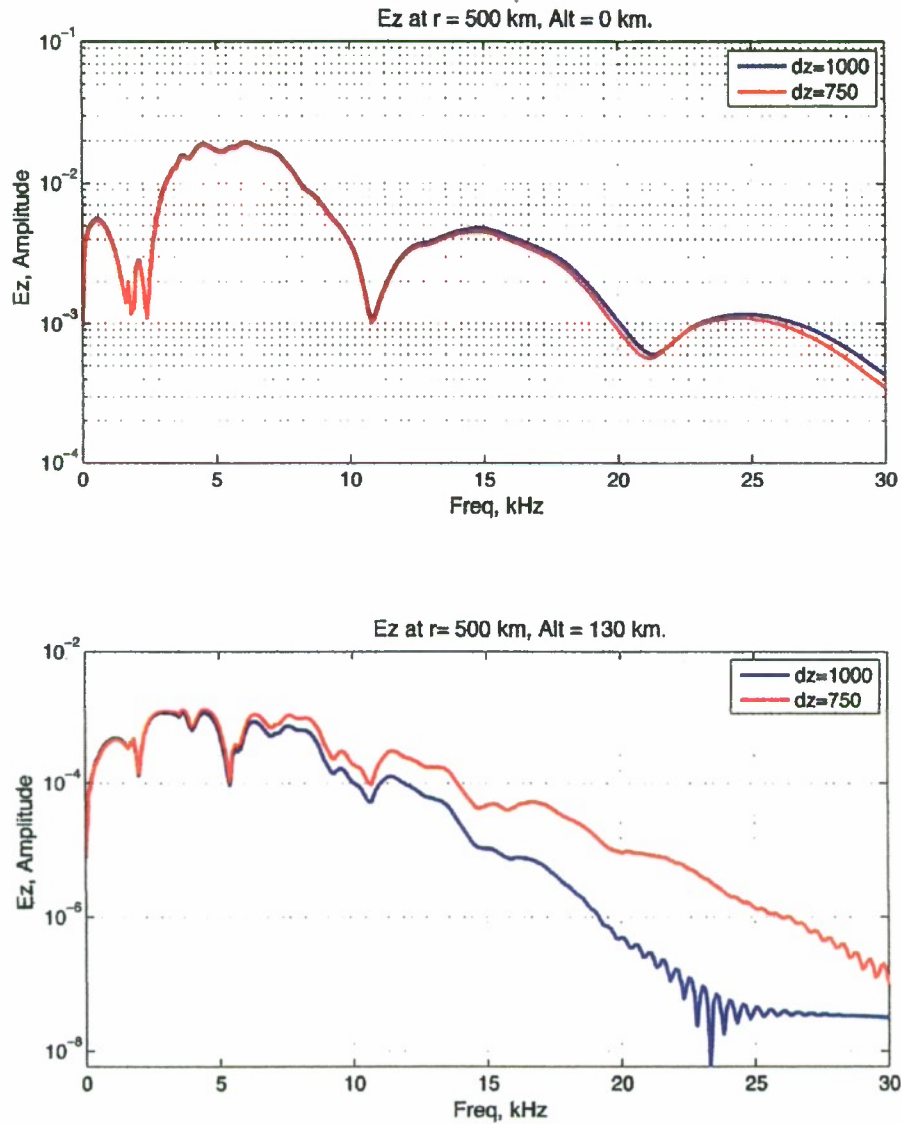


Figure 3. Test of FDTD model convergence from low-latitude NPM transmitter. The panels show the spectrum of low-altitude (top) and high-altitude (bottom) electric fields as the grid spacing in the simulation is reduced by 25%. The change in the low-altitude fields is almost negligible across the entire band, indicating that the results are accurate. However, the high-altitude fields differ somewhat above 5 kHz and differ enormously above 15 kHz.

4.3. High-Latitude vs. Low-Latitude Model Convergence—Complete Analysis

To quantify the connection between grid spacing, geomagnetic latitude, and simulation accuracy, we ran a series of simulations using parameters corresponding to the

NML (high latitude) and NPM (low latitude) transmitters with grid spacings of 1000, 500, and 250 meters. Finite difference simulations are guaranteed to eventually converge to the correct answer as this grid spacing is reduced, but it is not always easy to know what grid spacing is required to maintain errors below a specified level. We have found that, for a given uniform grid spacing, the low-altitude fields can be computed correctly while the high-altitude fields are dramatically incorrect. This shows that a nonuniform grid approach, in which low altitudes are resolved coarsely and only the highest altitudes are resolved finely, is the key to achieving efficient simulations of high-altitude fields. At high latitudes (i.e., NML), 500-m grid spacing results in fairly accurate high-altitude fields in the 20 – 25- Hz band. But at low latitudes (i.e., NPM), 250 m and smaller grid spacing is required to achieve the same accuracy. The convergence in all cases shows second-order accuracy, which is expected. This also means that correct answers can be estimated by extrapolating the convergence to its limit.

All of the figures below show the amplitude spectrum of one electric field component (the results are essentially identical for all E and H components) observed at 200-km range from the transmitter (short range is required for the simulations to be manageable for fine grids) and either 90-km (low) or 130-km (high) altitude. Figure 4 shows the low-altitude (90 km) field spectrum for a background magnetic field corresponding to the NML transmitter (high latitude) for 3 different grid spacings. The low-altitude fields are almost invariant to grid spacing, indicating that the solution has almost converged, even at 1-km spacing, and, consequently, that these results are all numerically correct. If we treat the 250-meter solution as “correct,” the bottom panel shows the relative error for 1-km and 0.5-km grids. These relative errors are all smaller than 10% except above roughly 30 kHz.

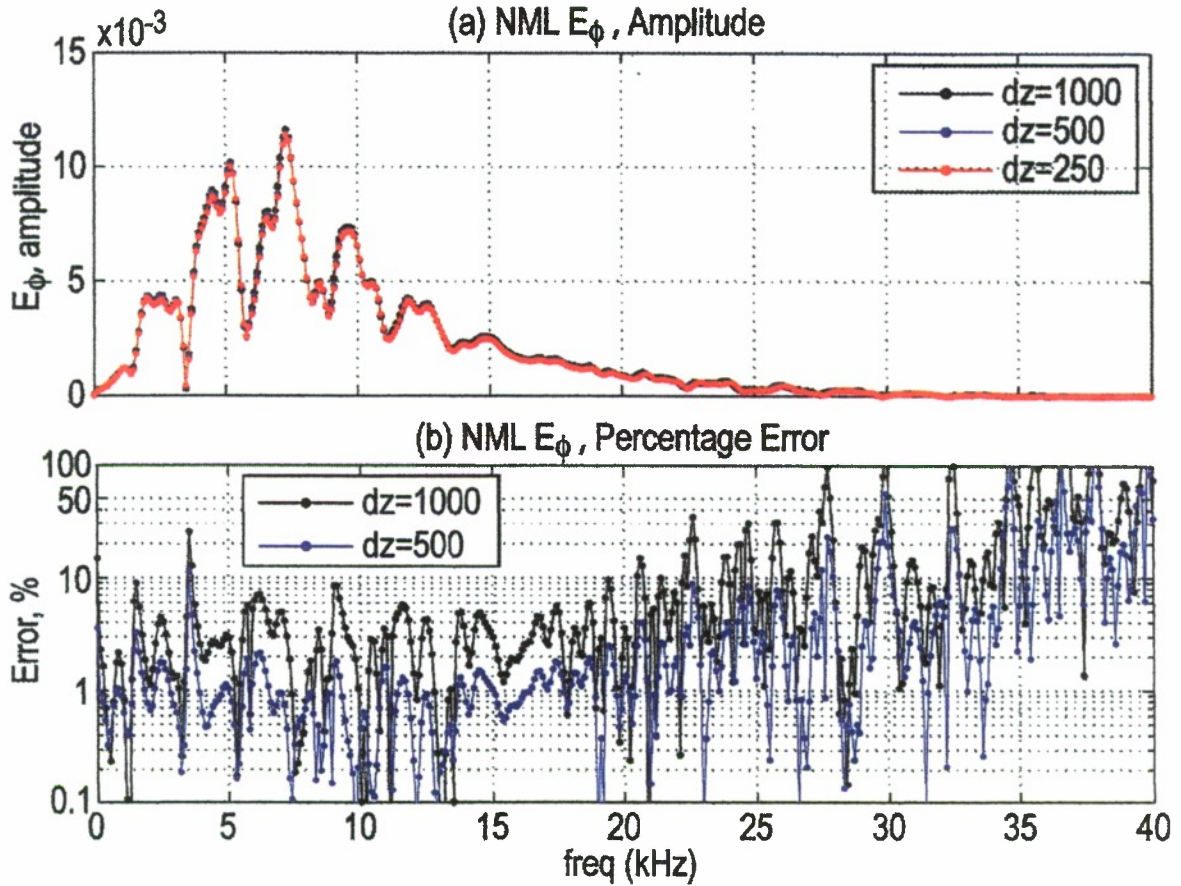


Figure 4. The low-altitude (90 km) field spectrum for a magnetic latitude corresponding to the NML transmitter (high latitude) for 3 different grid spacings.

Figure 5 shows the comparison for the same field component at 130-km altitude. At low frequencies (<10 kHz), the solution is nearly converged for 1-km grid spacing. But at higher frequencies, particularly the target frequencies of 20- to 30 kHz, a 1-km grid is not quite enough to give the right answer, as seen by the almost 50% change in the answer when the grid size is reduced from 1 km to 0.5 km. The step from 0.5 to 0.25 km, however, produces only a small change ($<10\%$) in the solution, indicating that by 0.5 km, the solution is almost correct even at high altitudes.

Figure 5 (and the other figures below) also shows clearly that the solution is converging with second-order convergence, in which the error shrinks in proportion to the square of the grid size. In other words, halving the grid spacing results in a 4x error reduction (see, for example, how the error drops from 40% to 10% at 20 kHz when the grid goes from 1 km to 0.5 km). This is as it should be, but it is always nice to get confirmation.

Importantly, because this convergence is well-understood mathematically, it can be exploited to estimate the “correct” answer from simulations that have not quite converged to the correct answer. This idea is called the “deferred approach to the limit”

and is used frequently in a variety of numerical calculations. For example, in the upper right panel, we can see that the fields are increasing steadily as the grid size is reduced, and we know that the error is decreasing by a factor of 4 for every halving of the grid size. Knowing this, the limit of this convergence can be estimated from simulations at only two grid sizes, each of which has not yet converged. In this way, the desired result can be obtained using relatively coarse and, therefore, much faster computations.

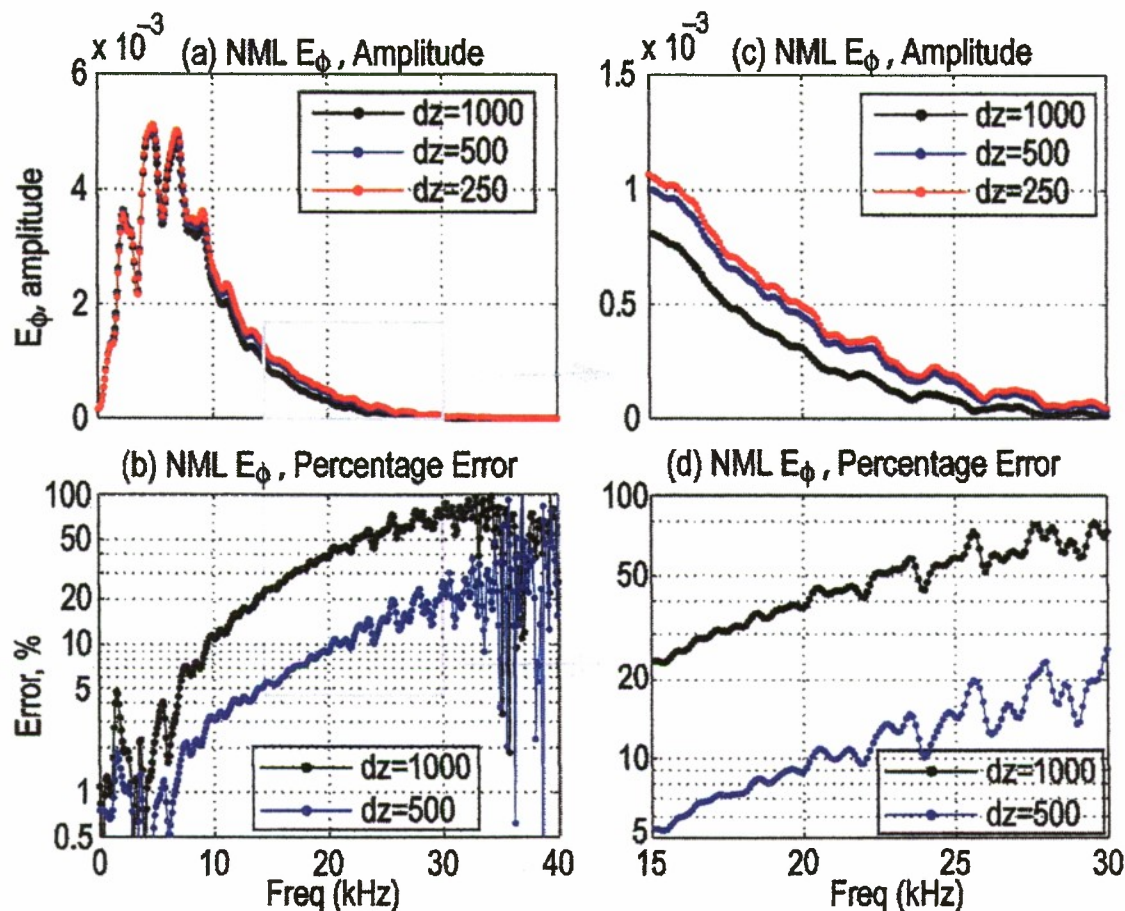


Figure 5. The high-altitude (130 km) field spectrum for a magnetic latitude corresponding to the NML transmitter (high latitude) for 3 different grid spacings.

The story is somewhat different for low-latitude transmitters, as we have already found and reported. Figure 6 shows, in the same format as Figure 4, the low-altitude (90 km) fields produced by the NPM transmitter. For the same sequence of grid spacings, the solution is not nearly as converged as was found for the high-latitude transmitter. A 500-meter grid is needed to reach the same relative error (1–2%) that a 1-km grid yielded for NML. Nevertheless, reasonably correct answers are obtained even for the larger grid spacings considered here. Note, again, the second-order convergence—for example, the error drops from 8% to 2% at about 17 kHz when the grid size is halved.

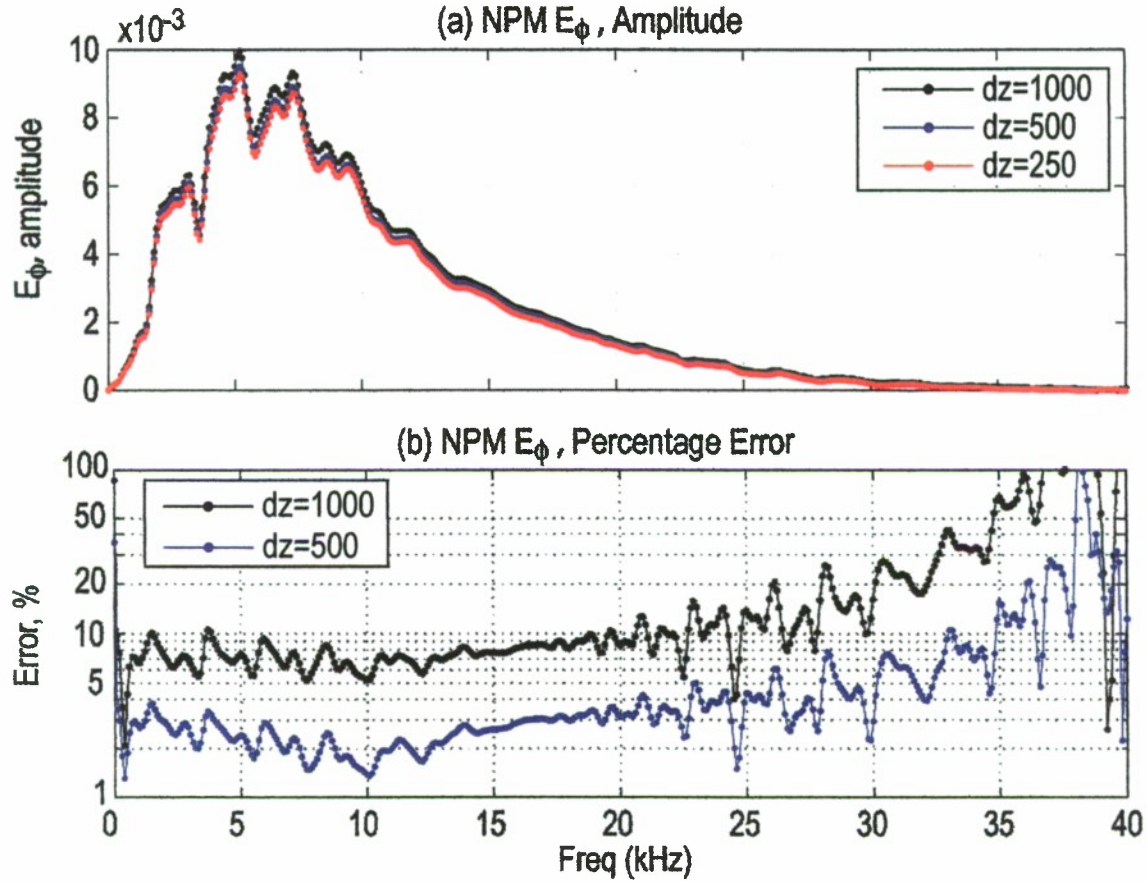


Figure 6. The low-altitude (90 km) field spectrum for a magnetic latitude corresponding to the NPM transmitter (low latitude) for 3 different grid spacings.

The convergence of the high-altitude fields is especially striking, as shown in Figure 7. Even though a 1-km grid yields the low-altitude (90 km) fields with reasonable accuracy up to 30 kHz, the high-altitude (130 km) fields are grossly underestimated above about 5 kHz for the same grid. The solution even changes significantly (about a factor of 2) when the grid size is reduced from 500 to 250 meters, indicating that an even finer grid is required for an answer close to convergence. We expect that the deferred approach to the limit described above may be especially valuable for these low-latitude cases in which the required grid spacing is fine.

Together, these results quantify rather precisely the relationship between grid size and error at both low- and high-latitudes and low- and high-altitudes. Importantly, they confirm that the computations that we have already reported for the high-latitude NML transmitter, which used a 1-km grid, are reasonably accurate but perhaps underestimate the high-altitude fields by roughly 30%.

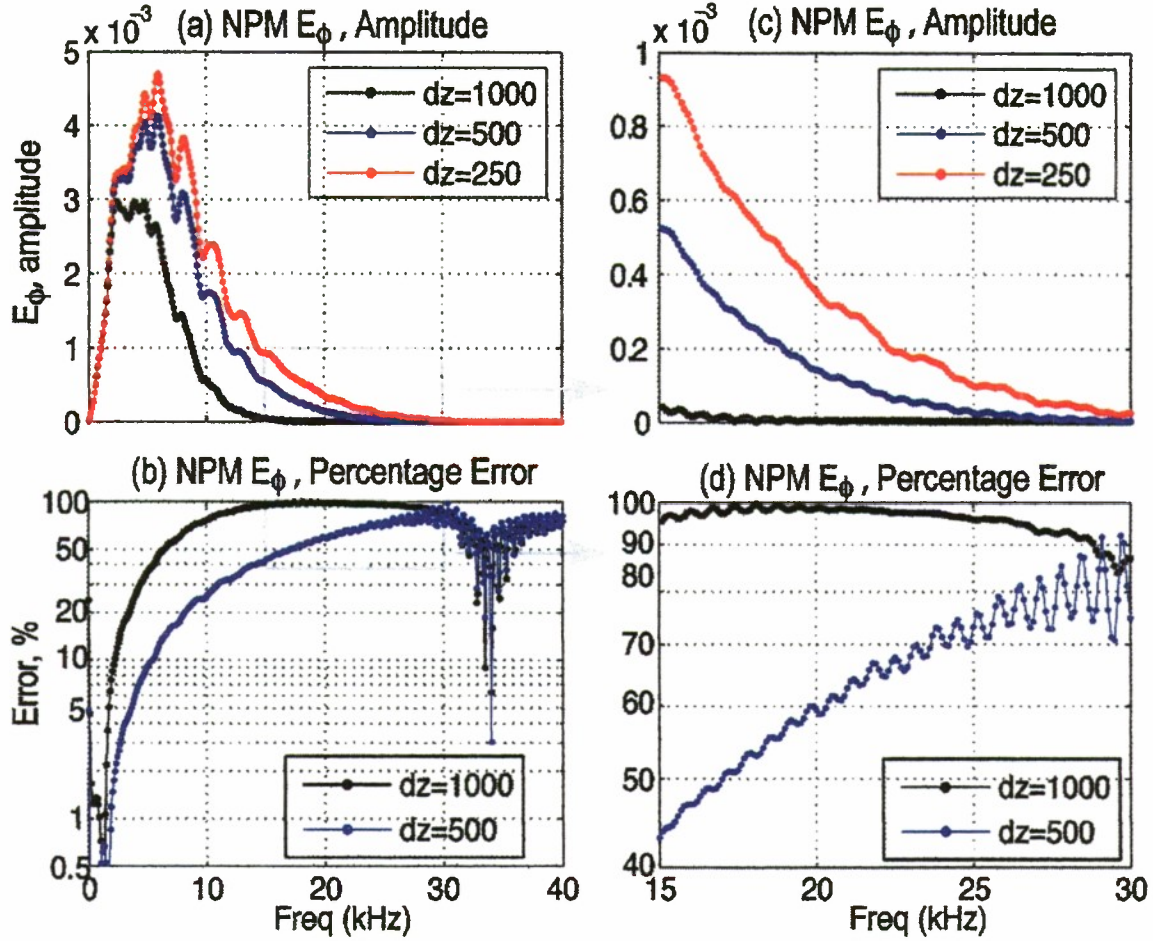


Figure 7. The high-altitude (130 km) field spectrum for a magnetic latitude corresponding to the NPM transmitter (low latitude) for 3 different grid spacings

4.4. Time Harmonic Code and Initial Results

As mentioned above, we are developing a time harmonic finite difference code to complement the time domain code that has produced the already-reported results from this project. A time harmonic code will have several advantages. For single frequency computations, it should be significantly faster than the time domain code. It also enables variable grid resolution that can be implemented easily, which should also increase model efficiency by letting fine grid spacing be used only where it is needed (high altitude, in general).

Here, we report results comparing frequency domain and time domain simulations for high-latitude locations. The plots that follow compare low-altitude (0 km) and high-altitude (130 km) VLF electric fields computed by the time domain code and the new frequency domain code. The frequency domain code is functional although it is still very much in development. Because of limitations of the Matlab matrix solvers, we use, in this preliminary version, the horizontal range of the simulations which is limited to about

100 km. Obviously, this is much shorter than we ultimately need, but we emphasize that this is purely a limitation on the solvers, not on the technique or even the code. Transitioning this code to other computers and solvers should be a very straightforward process. The simulations shown below are also for high-latitude sources for simplicity.

Figure 8 shows the vertical electric field vs. range at ground level for a 10-kHz source (radiated power is not important as long as the sources are identical in both simulations). The plot shows field amplitude for both frequency domain (FD) and time domain codes (TD) computed with two different levels of spatial discretization (500 m and 1000 m). Aside from some small discrepancies within 10 km of the source, the two are in excellent agreement. This also confirms that low-altitude fields are essentially converged at 1-km discretization.

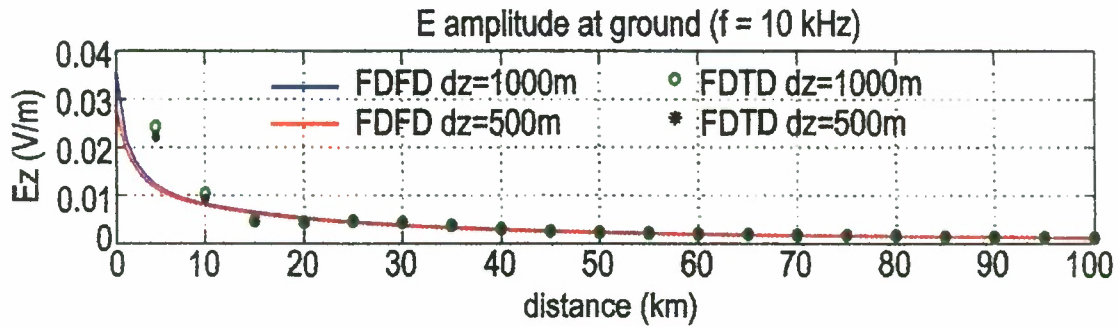


Figure 8. Low-altitude fields produced by a 10-kHz source computed using the FD and TD codes. The agreement is excellent, validating the new FD code.

Figure 9 shows all three electric field components at high altitude (130 km) for the same source computed with both codes. The FD code results change somewhat when the spatial discretization is reduced to 500 m, indicating that the simulation is not quite converged at 1000-m discretization. However, the 500-m TD and FD runs are again in excellent quantitative agreement, confirming the correctness of the FD simulation results. The component of E parallel to the background magnetic field (E_z , in this case) is much smaller than the other components, as expected. The two horizontal components have equal amplitudes (shown) and are in phase quadrature, showing that the upward traveling fields are circularly polarized, also as expected.

Figures 10 and 11 show the same comparisons except for a 20-kHz source frequency. The low-altitude fields agree well, which is consistent with the TD code convergence analysis. The high-altitude fields are generally in good quantitative agreement, but not to the same degree as the 10-kHz fields. The FD results also show a major change in the shape of the field profile from 1000-m to 500-m discretization. A further decrease in the FD discretization might be required for more quantitatively accurate results. The most important quantity, the general field amplitude, agrees well between the TD and FD code.

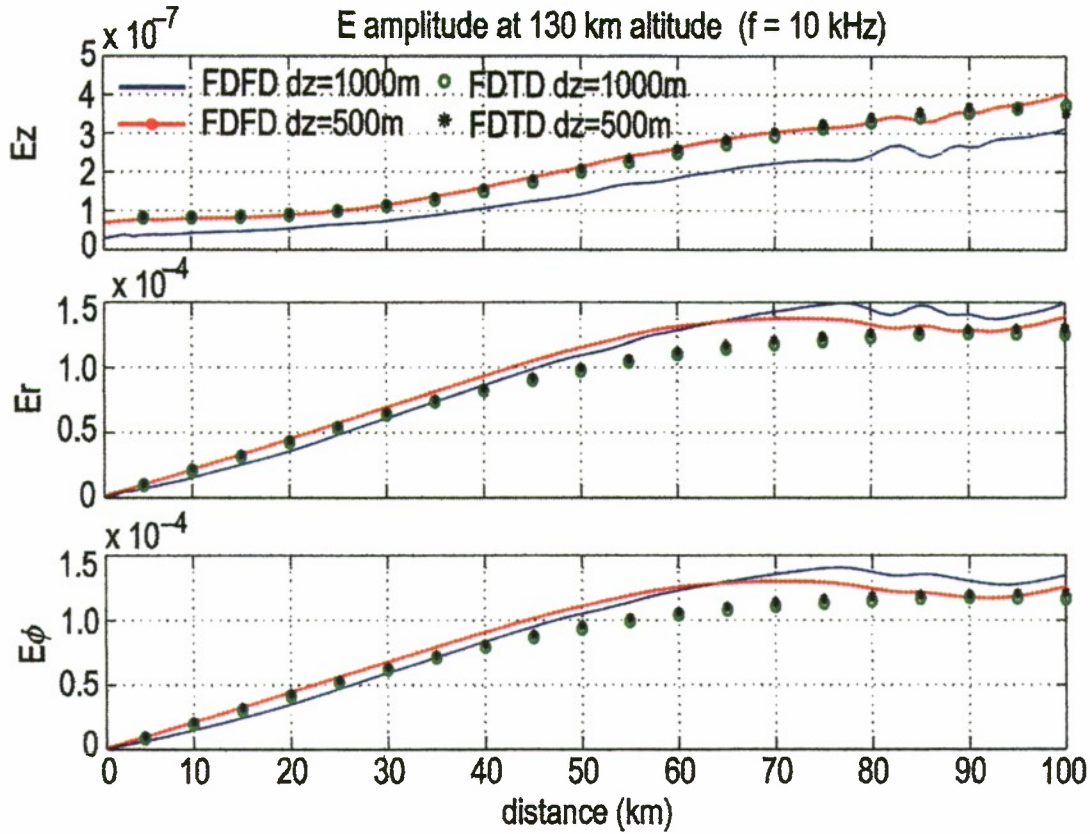


Figure 9. High-altitude fields produced by a 10-kHz source computed using the FD and TD codes. The agreement is again excellent.

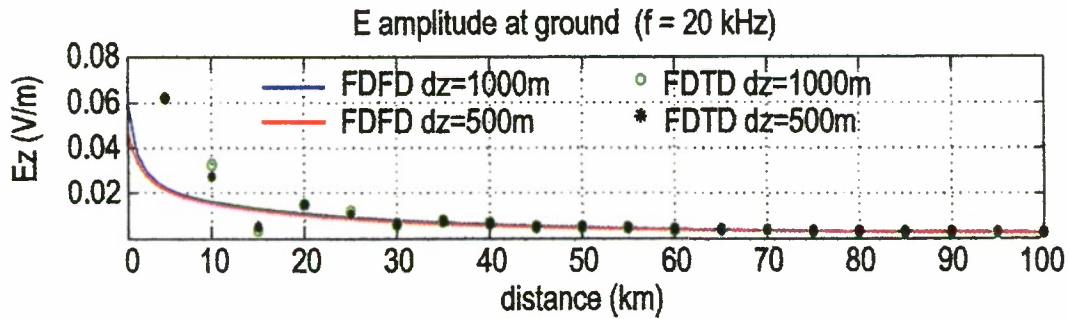


Figure 10. Low-altitude fields produced by a 20-kHz source computed using the FD and TD codes.

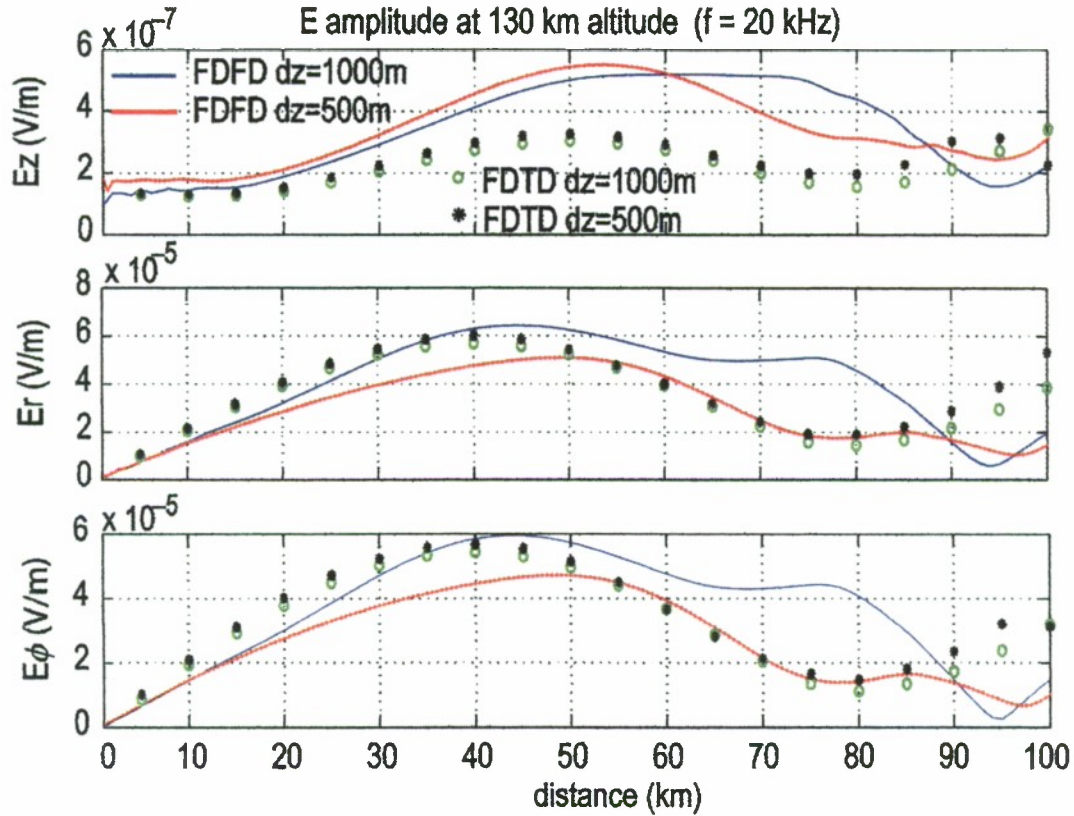


Figure 11. High-altitude fields produced by a 20-kHz source computed using the FD and TD codes.

The important difference between these codes is their speed, which is shown in Table 1. The TD code computes all frequencies simultaneously, which has some advantages for broadband fields but may not be maximally efficient if only one frequency or several frequencies are desired. The FD code computes the field for only one specific frequency, and is consequently faster. The two codes were run on comparable machines. Each code's absolute run time could be improved by running on faster platforms, but the ratio between the two should be relatively invariant.

Table 1. Comparison of TD and FD Code Run Times. The FD Code is Approximately 90 Times Faster

Code Type	Spatial Discretization	Run Time
TD	1000 m	1332 s
FD	1000 m	16 s
TD	500 m	9684 s
FD	500 m	129 s

As Table 1 shows, the FD code is approximately 90 times faster than the TD code for both discretizations. This is a major improvement and justifies our further effort in developing the FD code. We also emphasize that the FD code makes multiple grid scales relatively straightforward. This will also improve code efficiency by enabling us to place spatial resolution only where it is needed.

5. CONCLUSIONS

Despite challenges related to the arrival of funds to support this project, significant technical progress has been made. A complete end-to-end run of the high-altitude VLF power prediction model has been completed using our modeled 130-km altitude VLF power predictions as the input to the higher altitude ray-tracing code. This resulted in good agreement with high-altitude VLF field measurements from the IMAGE satellite. Previous end-to-end runs like this which used semi-empirical ionospheric penetration had revealed a ~20-dB discrepancy between the measured and predicted fields. Our model does not require any such correction factor and appears to show that this discrepancy originates in the ionospheric penetration calculation.

We also better understand the convergence and accuracy issues associated with the magnetic latitude of the source. A series of simulations using parameters corresponding to the NML (high latitude) and NPM (low latitude) transmitters with grid spacings of 1000, 500, and 250 meters showed that, for a given uniform grid spacing, the low-altitude fields can be computed correctly while the high-altitude fields are dramatically incorrect. This shows that a nonuniform grid approach, in which low altitudes are resolved coarsely and only the highest altitudes are resolved finely, is the key to achieving efficient simulations of high-altitude fields. At high latitudes (i.e., NML), 500-m grid spacing results in fairly accurate high-altitude fields in the 20 – 25-kHz band. But, at low latitudes (i.e., NPM), 250 m and smaller grid spacing is required to achieve the same accuracy. The convergence in all cases shows second-order accuracy, which is expected. This also means that correct answers can be estimated by extrapolating the convergence to its limit.

Lastly, the realization that very fine grid spacings are required to achieve accurate results at low latitudes has led us to develop a more efficient frequency domain (i.e., single frequency) VLF solver. Comparisons with results from the time domain code show that our preliminary frequency domain code gives answers in quantitative agreement with the time domain code but is about 90 times faster for single-frequency computations. This major enhancement in computational speed justifies the further development needed for this solver.

The ongoing code development will enable accurate predictions of the ionospheric wave fields and their statistical uncertainty. The end result will be the capability to predict more accurately the injection of VLF wave energy into the magnetosphere, which is a key component in the accurate modeling of the influence of VLF on natural radiation belt dynamics.

REFERENCES

- Budden, K. G., The propagation of Radio Waves, Cambridge Univ. Press, New York, 1985.
- Cummer, S. A., Modeling electromagnetic propagation in the Earth-ionosphere waveguide, *IEEE Transactions on Antennas and Propagation*, **48**, 1420-1429, 2000.
- Hu, W. and S. A. Cummer, An FDTD model for low and high altitude lightning-generated EM fields. *IEEE Transactions on Antennas and Propagation*, **54**, 1513–1522, 2006.
- Pappert, R. A. and J. A. Ferguson, VLF/ELF mode conversion model calculations for air to air transmission in the earth-ionosphere waveguide, *Radio Science*, **21**, 551, 1986.
- Taflove, A. and S. C. Hagness, Computational Electrodynamics: The Finite-Difference Time-Domain Method, Artech House, Norwood, Mass., 2000.

List of Symbols, Abbreviations, and Acronyms

AFRL	Air Force Research Laboratory
FDTD	Finite Difference Time Domain
LWPC	Long Wave Propagation Capability
NPML	Nearly Perfect Matched Layer
VLF	Very Low Frequency